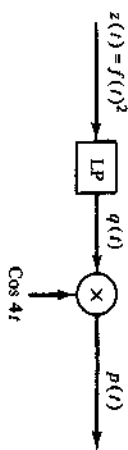


$Y_1(j\omega), Y_2(j\omega), Z_1(j\omega), Z_2(j\omega), w_1(t),$ and $w_2(t). Y(j\omega) \leftrightarrow y(t)$
 $z(t).$

Consider the following system:



The block labeled LP is an ideal low-pass filter with bandwidth $\omega_c = 2$ rad/sec. The input signal $f(t)$ has a Fourier transform $F(j\omega) = 10|t|(\omega + 2)$.

Determine and plot $Z(j\omega), Q(j\omega), P(j\omega),$ and $q(t).$

$$Z(j\omega) \leftrightarrow z(t), \quad Q(j\omega) \leftrightarrow q(t), \quad P(j\omega) \leftrightarrow p(t)$$

A low-pass filter has the system function:

$$H(j\omega) = \frac{10(10 + j\omega)}{(5 + j\omega)(20 + j\omega)}$$

Determine the cutoff frequency ω_c . Then normalize the frequency response $H(j\omega)$ by ω_c/ω_0 . Convert this normalized low-pass filter into a band-pass filter with $\omega_0 = 50$ and $\omega_1 = 40, \omega_2$ and ω_3 are respectively the upper and lower cutoff frequencies. Plot the magnitude of this band-pass filter.

The Discrete Fourier Transform and the Fast Fourier Transform

INTRODUCTION

In Section 8-6 we illustrated the essentials of the Fourier analysis by considering a number of applications. Most of these applications were from the communications area. Another area of engineering science that is becoming increasingly important is that of signal processing. Within this field, the digital or discrete Fourier transform is beginning to play a large role. Real signals, like radar tracks, which are often processed with the Fourier transform in order to reveal their spectral content, are typically measured at discrete points in time, resulting in discrete time signals, $f(n)$. These discrete or discretized time signals call for some kind of discrete Fourier transform (DFT).

Thus the need for a DFT arises from discrete signals. From a slightly different point of view, let us recall the definitions:

$$F(j\omega) = \int_{-\infty}^{\infty} f(t)e^{-j\omega t} dt \quad (9-1)$$

$$f(t) = \frac{1}{2\pi} \int_{-\infty}^{\infty} F(j\omega)e^{j\omega t} d\omega \quad (9-2)$$

The numerical computation of these integrals using digital computer processing requires that we take the continuous signals $f(t)$ and $F(j\omega)$ and discretize them. Also, we replace the integrals by finite summations. These manipulations lead directly to a discrete Fourier transform and an inverse discrete Fourier transform (IDFT). After a discussion of the DFT and the IDFT, we consider the problems of aliasing and leakage and the technique of windowing, all of which are relevant to the DFT. Then we investigate some of the DFT properties, after which we examine some efficient ways to compute the DFT and the IDFT.

The fast Fourier transform (FFT) is an efficient way of computing the DFT. Its efficiency results from a number of DFT mathematical operations. This is accomplished by exploiting the advantage of certain periodicities that appear in the DFT. In this section we focus on the development of two basic FFT algorithms: the decimation-in-time algorithm and the decimation-in-frequency algorithm.

This chapter, then, explores the mathematical basis of the DFT and the FFT. Although research into the theory and applications of the DFT and FFT has expanded considerably since the early 1970s, there is still an important research to be done in these areas and interested students are encouraged to consult the literature.

9-1 THE DISCRETE FOURIER TRANSFORM

Given $f(n)$, how do we determine its Fourier transform? The last chapter dealt only with continuous functions, $f(t)$. In order to arrive at a discrete Fourier transform, we follow a path that takes off from the theory of Fourier transforms and employs the duality property. Recall from Chapter 8 that a function is periodic

$$c_n = \frac{1}{T} \int_T f(t) e^{-jn\omega_0 t} dt$$

$$f(t) = \sum_{n=-\infty}^{\infty} c_n e^{jn\omega_0 t}$$

This is the complex exponential Fourier series representation and the series coefficients. This well-known pair can be represented as:

$$f(t) \leftrightarrow c_n$$

Corresponding to a periodic time function, we have a sequence of discrete frequency domain that are the discrete exponential Fourier coefficients.

Now if we start with a discrete function $f(n) = f(nT)$, then the discrete sequence of time points that are analogous to the discrete Fourier coefficients. Duality ideas suggest that corresponding to the discrete function $f(n)$ we would have a continuous frequency transform that is the frequency domain. This proves to be precisely the case.

Consider the transform pair:

$$f(t) \leftrightarrow F(j\omega)$$

To illustrate the development here, assume that we have an $f(t)$ and $F(j\omega)$ in Figure 9-1(a). The time function $f(t)$ is assumed to be time-limited outside the range $-\alpha \leq t \leq \alpha$. The transform $F(j\omega)$ is assumed to be band-limited: It is zero outside the range $-\beta \leq \omega \leq \beta$. Such assumptions are fictitious, of course, because any time-limited $f(t)$ like the trian-

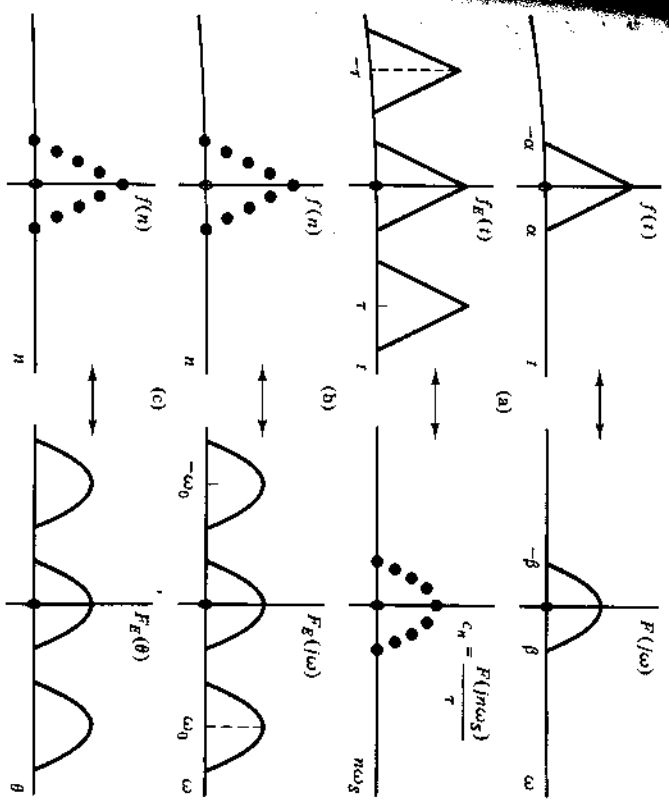


Figure 9-1 (a) Fourier transform pair; (b) periodic time function and discrete frequency function; (c) periodic frequency function and discrete time function; (d) same as (c) except frequency is normalized.

9-1(a) will always have a Fourier transform that is not band-limited. On the other hand, if $F(j\omega)$ is band-limited as in Figure 9-1(a), then the corresponding time function $f(t)$ will never be time-limited. Time-limiting and band-limiting are mutually exclusive phenomena. Although proving this in general is rather difficult, a glance at some of the famous Fourier transform pairs of the last chapter should be convincing. Note, for example, that the square pulse that is time-limited has a Sinc transform that is not band-limited. The consequences of the "useful fiction" to be employed in this development will be considered later.

Assume at first that $f(t)$ is not periodic. Now sample $F(j\omega)$ at $\omega = 0, \pm\omega_0, \pm 2\omega_0, \dots$. This yields $F(jn\omega_0)$, a discretized frequency domain function. Using this function, we can construct the frequency-domain points c_n which are actually the complex exponential Fourier series coefficients:

$$c_n = \frac{F(jn\omega_0)}{\tau} \tag{9-7}$$

Corresponding to these Fourier series coefficients we have $f_E(t)$, the periodic extension of the original $f(t)$, periodic with period τ . The functions $f_E(t)$ and c_n would appear as in Figure 9-1(b).

Next we employ duality and reverse the roles of $f_E(t)$ and c_n , the time-domain and frequency-domain functions. Instead of sampling $F(j\omega)$, we

Example $f(t)$ at $t = 0, \pm T, \pm 2T, \dots$. This yields $f(n) = f(nT)$. A sequence of points that in the time domain is analogous to a discrete-time sequence of Fourier series coefficients. Employing the concept of periodic extension, the functions $f(n)$ and $F_E(j\omega)$ would appear as in Figure 9-1. The function $F_E(j\omega)$ is periodic with period ω_0 and we can write:

$$F_E(j\omega) = \sum_{n=-\infty}^{\infty} \tilde{c}_n e^{-jn\omega T}$$

where $T = 2\pi/\omega_0$. Note that Equation 9-4 has a positive sign in the exponential. The negative sign in Equation 9-8 is due to the fact that argument reversal occurs in applying the duality property. Now let $\theta = \omega T$ and write:

$$F_E(\theta) = \sum_{n=-\infty}^{\infty} \tilde{c}_n e^{-jn\theta}$$

The Fourier series coefficients appearing in this equation are the samples of $f(t)$, that is:

$$\tilde{c}_n = f(nT) = f(n)$$

$$f(n) = \frac{1}{\omega_0} \int_{-\omega_0/2}^{\omega_0/2} F_E(j\omega) e^{jn\omega T} d\omega$$

Since $\omega = \theta/T$, we can write $d\omega = d\theta/T$.

$$f(n) = \frac{1}{2\pi} \int_{-\pi}^{\pi} F_E(\theta) e^{jn\theta} d\theta$$

$$F_E(\theta) = \sum_{n=-\infty}^{\infty} f(n) e^{-jn\theta}$$

Remember, $F_E(\theta)$ is periodic: $F_E(\theta + 2\pi) = F_E(\theta)$. Also, the variable is not ω but θ , where θ can be thought of as a normalized frequency. This reason, $F_E(\theta)$ is sometimes referred to as the "coordinate normalized transform." The functions $f(n)$ and $F_E(\theta)$ would appear as in Figure 9-2. Equations 9-12 and 9-13 constitute a discrete time Fourier transform pair. Equations 9-12 and 9-13 constitute a discrete time Fourier transform pair. Equations 9-12 and 9-13 constitute a discrete time Fourier transform pair. Equations 9-12 and 9-13 constitute a discrete time Fourier transform pair. Equations 9-12 and 9-13 constitute a discrete time Fourier transform pair.

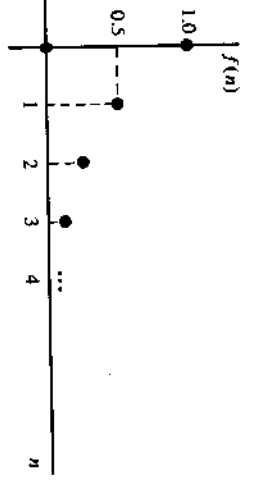


Figure 9-2 Sketch of $f(n)$ from Example 9-1.

EXAMPLE 9-1

Determine $F_E(\theta)$, the discrete time Fourier transform, for $f(n) = (\frac{1}{2})^n u(n)$. This function is sketched in Figure 9-2.

Solution

$$F_E(\theta) = \sum_{n=0}^{\infty} \left(\frac{1}{2}\right)^n e^{-jn\theta} = 1 + \frac{1}{2} e^{-j\theta} + \frac{1}{4} e^{-2j\theta} + \dots$$

$$= \frac{1}{1 - \frac{1}{2} e^{-j\theta}} = \frac{1}{1 - \frac{1}{2} \cos \theta + \frac{1}{2} j \sin \theta}$$

$$F_E(\theta) = |F_E(\theta)| \angle \arg F_E(\theta)$$

where $|F_E(\theta)| = \frac{1}{\sqrt{1.25 - \cos \theta}}$ and

$$\arg F_E(\theta) = -\tan^{-1} \left(\frac{\sin \theta}{2 - \cos \theta} \right)$$

The magnitude and phase are plotted separately in Figure 9-3. Both functions are periodic with period 2π .

It is interesting to note that in Equation 9-13 if we let $e^{j\theta} = z$, we get

$$F_E(\theta) |_{z=e^{j\theta}} = F_E(z) = \sum_{n=0}^{\infty} f(n) z^{-n} \tag{9-14}$$

which is none other than the two-sided Z transform. Thus all of the two-sided Z transform theory applies to the discrete time Fourier transform. To determine the discrete time Fourier transform for some $f(n)$, find the two-sided Z transform of $f(n)$ and simply let $z = e^{j\theta}$.

EXAMPLE 9-2

Determine $F_E(\theta)$ for $f(n) = (\frac{1}{3})^n \cos(n\pi) u(n)$ using the Z transform theory.

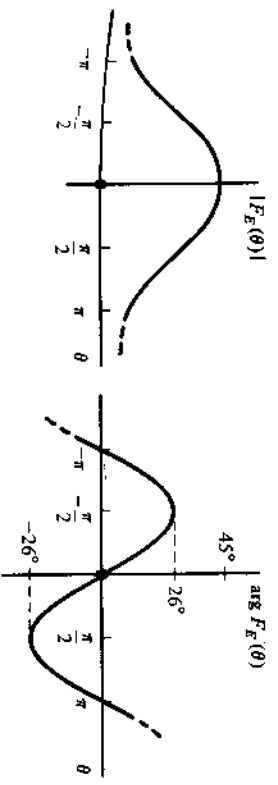


Figure 9-3 Magnitude and phase plots of the discrete time Fourier transform of $f(n) = (\frac{1}{3})^n u(n)$.

We assume that the inverse exists and avoid those cases where singular.

EXAMPLE 9-3

Determine \mathcal{W}^{-1} for the case of $N = 3$.

Solution

$$\mathcal{W} = \begin{bmatrix} 1 & 1 & 1 \\ 1 & W & W^2 \\ 1 & W^2 & W^4 \end{bmatrix} \quad \text{and} \quad W = e^{-j2\pi/3} = -\frac{1}{2} - j\frac{\sqrt{3}}{2}$$

$$\mathcal{W}^{-1} = \begin{bmatrix} W^5 - W^4 & W^2 - W^4 & W^2 - W \\ W^2 - W^4 & W^4 - 1 & 1 - W^2 \\ W^2 - W & 1 - W^2 & W - 1 \\ W^5 + 2W^2 - W - 2W^4 \end{bmatrix}$$

Dividing everything through by W^2 , we obtain:

$$\mathcal{W}^{-1} = \begin{bmatrix} W^2 - W & W^{-1} - W & W^{-1} - W^{-2} \\ W^{-1} - W & W - W^{-3} & W^{-3} - W^{-1} \\ W^{-1} - W^{-2} & W^{-3} - W^{-1} & W^{-2} - W^{-1} \\ W^2 + 2W^{-1} - W^{-2} - 2W \end{bmatrix}$$

Now

$$W = -\frac{1}{2} - j\frac{\sqrt{3}}{2}, \quad W^2 = -\frac{1}{2} + j\frac{\sqrt{3}}{2}, \quad W^3 = 1$$

$$W^{-1} = -\frac{1}{2} + j\frac{\sqrt{3}}{2}, \quad W^{-2} = -\frac{1}{2} - j\frac{\sqrt{3}}{2}, \quad W^{-3} = 1$$

Substituting in these values, we have:

$$\mathcal{W}^{-1} = \begin{bmatrix} j\sqrt{3} & j\sqrt{3} & j\sqrt{3} \\ j\sqrt{3} & -\frac{3}{2} - j\frac{\sqrt{3}}{2} & \frac{3}{2} - j\frac{\sqrt{3}}{2} \\ j\sqrt{3} & \frac{3}{2} - j\frac{\sqrt{3}}{2} & -\frac{3}{2} - j\frac{\sqrt{3}}{2} \end{bmatrix}$$

$$3j\sqrt{3}$$

$$= \frac{1}{3} \begin{bmatrix} 1 & 1 & 1 \\ 1 & -\frac{1}{2} + j\frac{\sqrt{3}}{2} & -\frac{1}{2} - j\frac{\sqrt{3}}{2} \\ 1 & -\frac{1}{2} - j\frac{\sqrt{3}}{2} & -\frac{1}{2} + j\frac{\sqrt{3}}{2} \end{bmatrix}$$

and this expression can be written as:

$$\mathcal{W}^{-1} = \frac{1}{3} \begin{bmatrix} W^0 & W^0 & W^0 \\ W^0 & W^{-1} & W^{-2} \\ W^0 & W^{-2} & W^{-4} \end{bmatrix}$$

Now, using induction, we can show that the result of Example 9-3 can be generalized for any N as:

$$\mathcal{W}^{-1} = \frac{1}{N} \begin{bmatrix} W^0 & W^0 & W^0 & \dots & W^{0(N-1)} \\ W^0 & W^{-1} & W^{-2} & \dots & W^{-(N-1)} \\ W^0 & W^{-2} & W^{-4} & \dots & W^{-2(N-1)} \\ \vdots & \vdots & \vdots & \ddots & \vdots \\ W^0 & W^{-(N-1)} & W^{-2(N-1)} & \dots & W^{-(N-1)(N-1)} \end{bmatrix} \quad (9-21)$$

Comparing this inverse to the matrix in Equation 9-18, we note that the only differences are the change in sign in the exponent of W and the multiplicative factor of $1/N$. The change in sign actually corresponds to taking a complex conjugate. Thus in view of Equation 9-16 and the matrices \mathcal{W} and \mathcal{W}^{-1} , we can write:

$$f(n) = \frac{1}{N} \sum_{k=0}^{N-1} F(k) e^{j(2\pi/N)kn} \quad (9-22)$$

This is the inverse DFT (IDFT). The DFT is expressed by Equation 9-16. The DFT pair can be indicated by the notation:

$$f(n) \leftrightarrow F(k) \quad (9-23)$$

Expressing Equation 9-23 in terms of W , we get:

$$F(k) = \sum_{n=0}^{N-1} f(n) W^{kn} \quad (9-24)$$

and

$$f(n) = \frac{1}{N} \sum_{k=0}^{N-1} F(k) W^{-kn} \quad (9-25)$$

the similarities are striking. The minus sign of W^{-kn} , again, conjugation. Except for this and the factor of $1/N$, the forms of DFT are identical.

9-2 ALIASING AND LEAKAGE PROBLEMS

So far we have illustrated the theory by using the fiction of a band-limited signal. Actual physical signals, however, are time-limited from a radar trace, for example, must start at some finite time t_1 and terminate at time t_2 . Time-limited signals, in reality, are never band-limited. $F(j\omega)$ might appear as in Figure 9-5(a) and, consequently, $F(k)$ will appear as in Figure 9-5(b). The overlap in $F(k)$ produces a phenomenon called aliasing. An alias is something that stands for something else, like an assassin who takes the place of an actual name. For our purposes, aliasing reveals that frequency components that substitute for other frequency components. Figure 9-5(b) reveals that at a frequency slightly below W , for instance, a frequency component standing in for the component that would be there if no overlap occurred. The actual value at that frequency is the contribution from the original unaliased spectrum plus a term from a component slightly above W . With aliasing, information is lost. The phenomenon can be minimized, as we have seen in Chapter 8, by sampling the original $f(t)$ at a sufficiently high sampling rate. The sampling rate that we should sample at a frequency at least twice the highest frequency $F(j\omega)$. If $F(j\omega)$ is band-limited, there is some finite band-limited. If $F(j\omega)$ is not band-limited, there is some finite band-limited. But, again, $F(j\omega)$ is, in reality, never band-limited. We need to sample at an infinite frequency to avoid overlap. What is the consequence of sampling as fast as possible within the hardware constraints and the inevitable aliasing to a minimum. We could also use a low-pass filter

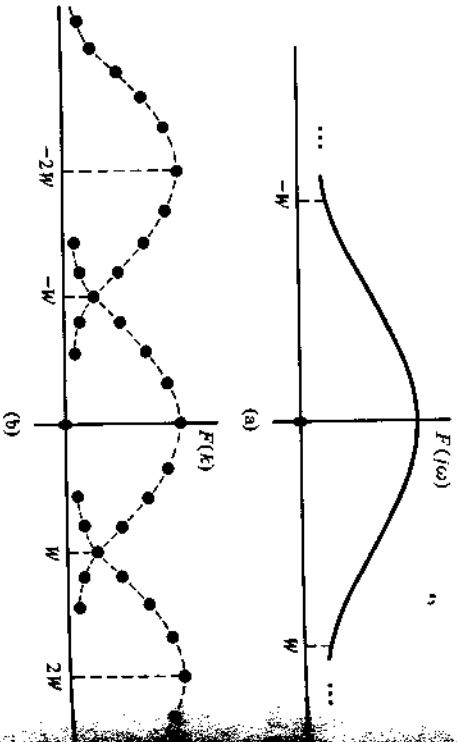


Figure 9-5 (a) Non-band-limited spectrum; (b) overlap in the DFT spectrum

signal prior to sampling. This would reduce overlap by producing a spectrum with sharper roll-off.

Another DFT problem closely tied to the aliasing problem is that of leakage. Both these problems are rooted in the time-limited nature of real physical signals. The abrupt discontinuities in time-domain signals due to starting and stopping a data record produce frequency spectra that typically have main-lobes containing most of the spectral information, as well as side-lobes in which information is lost. Side-lobes are spurious frequency peaks that detract from information contained in the main-lobe. Minimizing the side-lobes will minimize the information that is lost in the side-lobes. The information lost in the side-lobes is called leakage. The standard method of side-lobe minimization employs the technique of windowing. Windowing smooths the abruptness of data record discontinuities.

How does the idea of windows fit here? A window not only limits a view but frames and shapes it as well. The data are always cut off or framed by a window. The phenomenon x under observation is observed from some time t_1 to some time t_2 . In a typical DFT processing event, a signal x is available from t_1 to t_2 ; $x(t)$ to $x(n)$. In a discrete setting we can arrange these values as $x(n)$ from $n = 0$ to $N - 1$. Before delving too far into the discrete theory here, let us consider an example from continuous time. Continuous time representations seem to have a larger appeal to the uninitiated imagination. We will return shortly to the discrete world. This particular example is very simple, but nicely illustrates the general theory.

EXAMPLE 9-4

Given:

$$g(t) = \cos \omega_0 t \leftrightarrow G(j\omega) = \pi [\delta(\omega - \omega_0) + \delta(\omega + \omega_0)]$$

Let $w(t)$ be the unity gain square pulse:

$$w(t) = u(t + T) - u(t - T)$$

where

$$W(j\omega) = 2 \frac{\sin \omega T}{\omega}$$

Solution. Then $f(t) = g(t)w(t)$ can be considered to be a "windowed" version of $g(t)$. $f(t)$ is a truncated cosine. This could be a data record over a finite time interval of a pure cosine function. Taking the Fourier transform of $f(t)$, we would convolve $G(j\omega)$ and $W(j\omega)$ to get:

$$F(j\omega) = \left[\frac{\sin(\omega - \omega_0)T}{\omega - \omega_0} + \frac{\sin(\omega + \omega_0)T}{\omega + \omega_0} \right]$$

Note the plots of $G(j\omega)$, $W(j\omega)$, and $F(j\omega)$ in Figure 9-6. The effect of the window is to replace the impulses of the original function with transforms shaped like the transform of the window ($\sin x/x$), except that they are located at the points where the impulses occur. Looking only at $F(j\omega)$, we can deduce the presence of a sinusoid at $\omega = \omega_0$ in this simple case. The

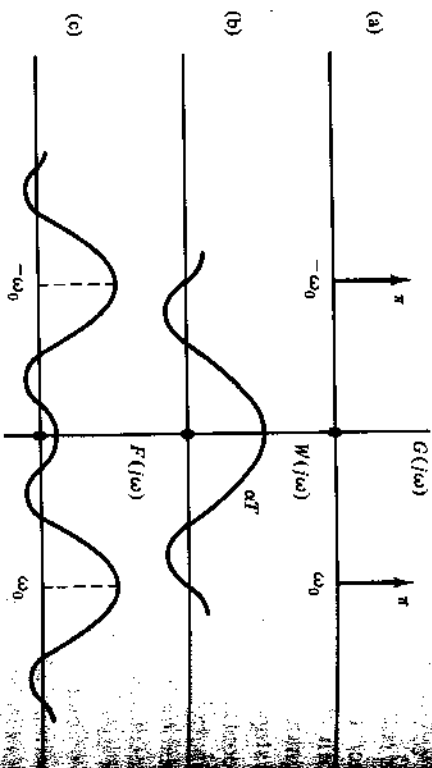


Figure 9-6 (a) Unwindowed Fourier transform; (b) transform of the windowed function.

$F(j\omega)$ function peaks at exactly those frequencies, $\pm\omega_0$, where its impulses. However, if $g(t)$ were composed of a sum of many different frequencies, then $F(j\omega)$ would consist of many shapes centered at these different frequencies. The overall becomes obvious. The peak value of one $\text{Sin } x/x$ term, for example, is so small that it gets lost in the side-lobes of a neighbor. Frequencies and amplitudes of the sinusoids in $g(t)$ from a real field of signal processing. One straightforward tactic to increase of estimating the sinusoids in $g(t)$ is to modify the window such that its transform is sharper or has lower side-lobes. $w(t)$ were chosen to be a triangle pulse instead of the square transform takes the form $(\text{Sin } x/x)^2$ which has lower side-lobes. $\text{Sin } x/x$. Many different windows have been proposed. Some be considered shortly.

Now in the discrete world, let us assume we have sample record $f(n)$, $n = 0, 1, \dots, N - 1$. We could employ Equation 9-10 the DFT without further ado. This would correspond to using a rectangular window $w(n) = 1, n = 0, 1, \dots, N - 1$. Then $f(n)$ where $g(n)$ is the actual time function that in principle could extend minus to plus infinity. Data from an actual finite time record gathered as $g(n)$ from $n = 0$ to $n = N - 1$. Without windowing, however, it is advantageous to employ nonuniform windows, especially window, we would just let $f(n)$ be these $g(n)$ values. As Example however, it is advantageous to employ nonuniform windows, especially to know the spectral content of a signal. If a triangular window, for example, then the first points in the data record are weighted more heavily than the last points are also weighted. This illustrates this weighting procedure, consider the following example.

9-2 ALIASING AND LEAKAGE PROBLEMS

EXAMPLE 9-5

Given:

$$g(n) = [\dots, 5, 2, 1, 4, 3, 4, 2, 2, 1, 1, 2, 1, 1, 0, 2, \dots]$$

is a data record to be processed from $n = 0$ to $n = 8$. Employ a triangular weighting

$$w(n) = [0.00, 0.25, 0.50, 0.75, 1.00, 0.75, 0.50, 0.25, 0.00]$$

Determine the values of $f(n)$ to be processed.

Solution. The values of $f(n)$ to be processed are $f(n) = g(n)w(n)$.

$$\text{Thus } f(n) = [0.00, 0.75, 2.00, 1.50, 2.00, 0.75, 0.50, 0.50, 0.00]$$

Now to consider some of the more common windows, assume that $w(n)$ is an even function with the origin as the point of symmetry. Since there is a point at $n = 0$, evenness will require an odd number of points for discrete window functions. However, we assume that $f(n)$ has an even number of points. This turns out to be convenient for the fast Fourier transform development that occurs later in the chapter. We also assume, in fact, that $N = 2^P$ where P is an integer. It seems problematic to have $w(n)$ with an odd number of points and $f(n)$ with an even number of points. This even-odd problem is resolved by recalling that $w(n)$ is a periodically extended function so that its first and last points are the same. Therefore we consider windows centered about the origin and having $N + 1$ points, where N is even. Then in an actual problem, since $w(n)$ is periodic, it can be shifted such that its left point coincides with the origin and the right point can be deleted. Remember that such a shift only contributes a phase shift term and leaves the magnitude of the frequency response unaffected.

In addition to the square and triangular windows, some of the other frequently used windows are: the Hann window, the Hamming window, the Gaussian window, the Blackman window, and the Dolph-Chebyshev window. There are also many varieties within these basic types. Since we must keep our discussion brief, we examine only a few of these.

9-2-1 The Hann Window

Analytically this window is described by the equation:

$$w(n) = 0.5 + 0.5 \cos \frac{2n\pi}{N}, \quad n = \frac{-N}{2}, \dots, -1, 0, 1, \dots, \frac{N}{2} - 1 \quad (9-26)$$

These kinds of windows are sometimes called "cosine on a pedestal" windows. The cosine is superimposed on a uniform or rectangular window. The result of

this configuration is very low side-lobes in the frequency domain. We can see this if the Hann window is compared to the rectangular $\text{Sin } x/x$ pattern of the rectangular window. The Hann window produces a series of side lobes that are displaced from the origin in such a way that their peaks are the side-lobe terms in the "pedestal" part of the Hann window. This is not merely superposition.

EXAMPLE 9-6

Determine and plot the DFT for the Hann window if $N = 8$. Compare the results to the DFT for a corresponding rectangular window.

Solution. For the Hann window, let us first plot $w(n)$ shifted to the left point coincides with the origin.

Let:

$$\bar{w}(n) = 0.5 + 0.5 \cos \frac{n\pi}{4}, \quad n = -4, -3, -2, -1, 0, 1, 2, 3, 4$$

which we plot as in Figure 9-7(a). Now shift $\bar{w}(n)$ to the right to form $w(n)$ as in Figure 9-7(b). Using $w(n)$, we compute the DFT

$$\begin{aligned} W(k) &= \sum_{n=0}^7 w(n) W^{nk}, & \text{where } W &= e^{-j(2\pi/N)} \\ &= e^{-j(\pi/n)} = \frac{1-j}{\sqrt{2}} \end{aligned}$$

$$\begin{aligned} W(0) &= 4.00 & W(2) &= W(3) = W(4) = W(5) = W(6) \\ W(1) &= -2.0 & W(7) &= -2.0 \end{aligned}$$

And since these functions are periodic, $W(8) = 4$, and so on. $W(k)$ as in Figure 9-8. Now for the rectangular window, let $w(n) = 1, 1, \dots, 7$.

$$\begin{aligned} W_R(k) &= 8, & k &= 0 \\ &= 0, & k &= 1, 2, 3, 4, 5, 6, 7 \end{aligned}$$

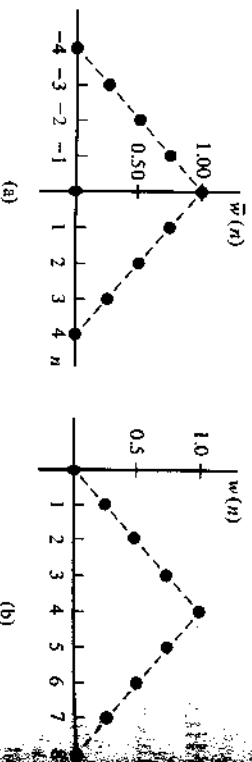


Figure 9-7 (a) Plot of Hann window for $N = 8$; (b) Hann window shifted.

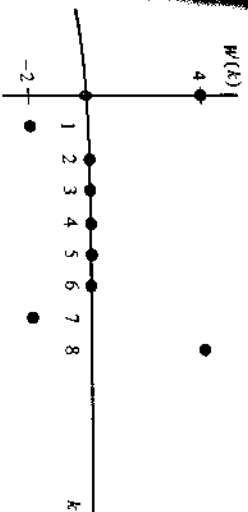


Figure 9-8 Plot of DFT for the Hann window.

We plot $W_R(k)$ as in Figure 9-9. Now observing the DFT plots in Figures 9-8 and 9-9, we seem to have results that contradict our discussion of the Hann window. From Figure 9-8, it appears that the Hann window exhibits some side-lobe behavior due to the values of -2.0 at $k = 1$ and $k = 7$. The rectangular window DFT in Figure 9-9 appears to exhibit no side-lobes at all. Why is there a discrepancy? The DFT of the rectangular window seems to have no side-lobes because the sample rate is such that we sample exactly at the zeros of the actual rectangular DFT. We know the rectangular window has a $\text{Sin } x/x$ type transform. These patterns do have rather large side-lobe levels.

If instead of computing $W(k)$ for these two windows we were to first determine $W(\theta)$ and plot $W(\theta)$ versus θ , then we would see the side-lobes displayed in a continuous fashion. $W(\theta)$ for the Hann window and $W_R(\theta)$ for the rectangular window would appear as in Figure 9-10. Notice that the main-lobe for the Hann window is wider than the main-lobe for the rectangular window. The side-lobes for the Hann window, however, are very low.

Before we leave this Hann window to consider some other windows, a few general comments are in order. For small values of N (like $N = 8$) we should not expect $W(\theta)$ and $W(k)$ to be very similar. But since θ is sampled at $\theta = 2\pi k/N$, for very large values of N , the number of sample values of $W(\theta)$ in the range $-\pi < \theta < \pi$ becomes very large as well. Thus $W(k)$ should look more like $W(\theta)$ for large N . Now sometimes the side-lobes in these windows are reduced so much that they hardly appear at all on a linear plot of $W(k)$ or $W(\theta)$. For this reason a dB scale is often used to plot the DFT magnitudes. The dB level of the first or largest side-lobe is often used as a measure of window quality. But since lowering

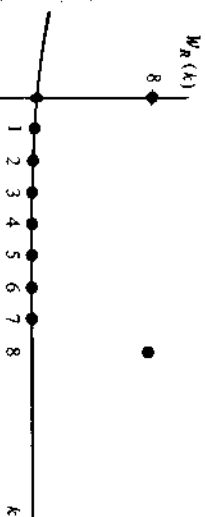
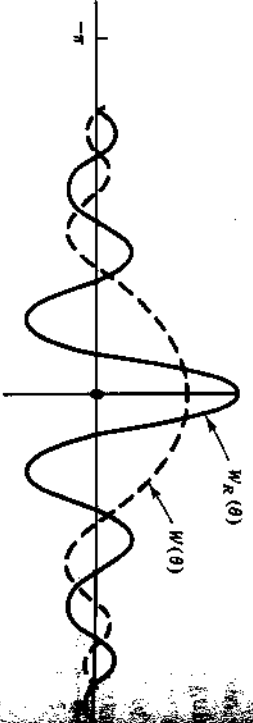


Figure 9-9 Plot of DFT for the rectangular window.

Figure 9-10 Plots of $W(\theta)$ and $W_R(\theta)$, the Hann and rectangle windows.

the side-lobes increases the width of the main-lobe, trade-offs are always necessary. The most useful windows in practice appear to be exhibiting 60 dB or more side-lobe suppression while at the same time exhibiting a main-lobe width that does not exceed about four times the rectangular window's main-lobe. For comparison purposes, the Hann window for large N exhibits a first side-lobe level of approximately 32 dB from the main-lobe and the Hann window has a first side-lobe of 31 dB.

9-2-2 The Gaussian Window

This window appears like a bell-shaped Gaussian distribution in the discrete time domain. The exact shape of the Gaussian window is a standard deviation parameter. One particular Gaussian window is the equation:

$$w(n) = \exp(-4.5(2n/N)^2), \quad n = \frac{-N}{2}, \dots, -1, 0, 1, \dots, \frac{N}{2}$$

Compared to the Hann window, this Gaussian window has lower side-lobes approximately 55 dB down—but has a wider main-lobe.

9-2-3 The Dolph-Chebyshev Window

This window is unique in that it provides uniform side-lobes and a minimum main-lobe width for a specified side-lobe level and specified data points. The use of this window in the signal processing area is common out of the radar design area. Radar designers have used this windowing in the design of linear phased arrays. The current design of the face of a phased array forms a Fourier transform pair with the pattern produced by the phased array radar. Dolph-Chebyshev windows have been used in this context for many years.

Now the analytical description of the Dolph-Chebyshev window is rather complicated because, in general, it employs Chebyshev polynomials. These polynomials can be expressed by the equation:

$$T_m(w) = \cos(m \cos^{-1} w)$$

Then, for example:

$$T_4(w) = 1 - 8w^2 + 8w^4$$

For a particular case in which we want side-lobe levels of 30 dB down from the main-lobe and for which we have $N = 100$ data points, we can write the DFT of the Dolph-Chebyshev window as follows:

$$W(k) = \cos \left(100 \cos k^{-1} \left(\cos \frac{k\pi}{50} \right) \right) \quad (9-29)$$

In general, the use of any of these windows will increase the chances of estimating the frequencies and amplitudes of sinusoids contained in a given data record. Which window should one use? There is no straightforward answer to this question.

Sometimes different windows are used with the same data record to see which window yields the minimal leakage. Occasionally, knowing beforehand what the data record is like will dictate the proper window. Because of these ambiguities, window selection is often considered more an art than a science. To conclude this window discussion, we note that the use of windowing occurs not only in DFT spectral estimation but in other areas as well, in particular, in the design and analysis of digital filters.

Aliasing and leakage are the most serious DFT problems. The ideal, of course, would be to have the DFT be equivalent to the continuous Fourier transform. We must content ourselves, however, with approximations. Aliasing and leakage corrupt our approximations. In this section we indicated the best way to deal with these corruptions. To eliminate the corruption due to aliasing, we need to sample the original signal at a rate greater than twice the highest frequency in the signal. Often this frequency is not known, in which case we sample at the highest practical rate. To deal with leakage, use windows. The more sophisticated windows require more computation time. As in most engineering problems, trade-offs are in order.

Assume now that we have $f(n)$ in hand. These data points have been gathered at the highest possible sampling rate and windowing has been done. We are ready then to return to Equations 9-24 and 9-25. To assist in the performance of the DFT and inverse DFT operations, we can employ a number of DFT properties. We will consider these next.

9-3 DFT PROPERTIES

Like the continuous Fourier transform of the previous chapter, there are a number of properties of the DFT that can facilitate some analytical tasks. The most important of the DFT properties are summarized in Table 9-1. Since a number of operations relating different time functions or different frequency functions are involved, we consider only two functions, $x(n)$ and $y(n)$, which have DFTs $X(k)$ and $Y(k)$, respectively.

TABLE 9-1 DFT PROPERTIES

Property	Data sequence representation	
Discrete Fourier transform	$x(n)$	$X(k)$
Linearity	$ax(n) + by(n)$	$aX(k) + bY(k)$
Periodicity of data and transform sequences	$x(n + lN), l, m = \dots, -1, 0, 1, \dots$	$X(k)$
Horizontal axis sign change	$x(-n)$	$X^*(k)$
Complex conjugation	$x^*(n)$	$X(-k)$
Data sequence sample shift	$x(n \pm n_0)$	$X(k) e^{\pm j2\pi k n_0 / N}$
Angle sideband modulation	$e^{j2\pi k_0 n / N} x(n)$	$X(k - k_0)$
Double sideband modulation	$[\cos(2\pi k_0 n / N)] x(n)$	$\frac{1}{2}[X(k - k_0) + X(k + k_0)]$
Data sequence circular convolution	$x(n) * y(n)$	$X(k)Y(k)$
Transform sequence circular convolution	$x(n)y(n)$	$X(k)Y(N - k)$
Arithmetic correlation	$x(n) * y^*(-n)$	$X(k)Y^*(k)$
Autocorrelation	$x(n) * x^*(-n)$	$ X(k) ^2$
Data sequence convolution	$\tilde{x}(n) * \tilde{y}(n)$ (augmented sequences)	$\tilde{X}(k) * \tilde{Y}(k)$ (augmented sequences)
Transform sequence convolution	$\tilde{x}(n)\tilde{y}(n)$	$\tilde{X}(k)\tilde{Y}(k)$
Symmetry	$(1/N)X(k)$	$x(n)$
Parseval's theorem	$\sum_{n=0}^{N-1} x(n) ^2$	equals $\frac{1}{N} \sum_{k=0}^{N-1} X(k) ^2$

Now since many of the DFT properties are very similar to the continuous Fourier transform presented in Chapter 8, we consider a few of the more important ones. These will be illustrated by example.

EXAMPLE 9-7

Demonstrate the periodicity of the DFT.

Solution. Let:

$$X(k) = \sum_{n=0}^{N-1} x(n)W^{nk}$$

be the DFT of $x(n)$,

$$\text{then } X(k + mN) = \sum_{n=0}^{N-1} x(n)W^{(k+mN)n} = \sum_{n=0}^{N-1} x(n)W^{kn}$$

$$\text{but } W^{mN} = e^{-j(2\pi/N)mN} = e^{-j2\pi mn}$$

which equals 1 as long as mn is an integer. Since n is an integer if m is an integer.

Therefore $X(k + mN) = X(k)$, for all $m = \dots, -1, 0, 1, 2, \dots$ that is, the DFT is periodic with period N .

EXAMPLE 9-8

Determine the DFT for $x(n) = [4, 3, 2, 1]$ and $N = 4$. Then demonstrate the horizontal axis sign change property and use it to determine the DFT for

$$y(n) = 4\delta(n) + 3\delta(n+1) + 2\delta(n+2) + \delta(n+3) \quad \text{where } N = 4.$$

Solution

$$x(n) \leftrightarrow X(k) = \sum_{n=0}^{N-1} x(n)W^{nk} = \text{DFT}[x(n)]$$

$$\text{DFT}[x(-n)] = \sum_{n=0}^{N-1} x(-n)W^{nk}$$

Letting $n = -m$, we get:

$$\text{DFT}[x(-n)] = \sum_{m=0}^{1-N} x(m)W^{-mk}$$

If we let $N = 8$ and expand this summation, we obtain:

$$\text{DFT}[x(-n)] = x(0)W^0 + x(-1)W^k + \dots + x(-7)W^{7k}$$

But recall that $x(n)$ and W^{nk} are periodic:

$$W = e^{-j(2\pi/N)} = e^{-j(\pi/4)}$$

in this case

$$W^{7k} = W^{-k}, W^{6k} = W^{-2k}, \dots, W^k = W^{-7k}$$

Also, we can write $x(-1) = x(7), x(-2) = x(6), \dots, x(-7) = x(1)$.

$$\begin{aligned} \text{Therefore } \text{DFT}[x(-n)] &= x(0)W^0 + x(1)W^{-k} + x(2)W^{-2k} \\ &+ \dots + x(N-1)W^{-k(N-1)} \\ &= \sum_{n=0}^{N-1} x(n)W^{-nk} \end{aligned}$$

and comparing this with $X(k)$, we write:

$$\text{DFT}[x(-n)] = X(-k)$$

therefore $x(-n) \leftrightarrow X(-k)$

Now for $x(n) = [4, 3, 2, 1]$ and $N = 4$,

$$W = e^{-j(\pi/2)} = -j$$

$$\begin{aligned} X(k) &= \sum_{n=0}^3 x(n)W^{nk} = x(0)W^0 \\ &+ x(1)W^k + x(2)W^{2k} + x(3)W^{3k} \end{aligned}$$